Antimicrobial activity of poly(vinyl alcohol)-poly(acrylic acid) electrospun nanofibers

Please, cite as follows:

Javier Santiago-Morales, Georgiana Amariei, Pedro Letón, Roberto Rosal, Antimicrobial activity of poly(vinyl alcohol)-poly(acrylic acid) electrospun nanofibers, Colloids and Surfaces B: Biointerfaces, Volume 146, 1 October 2016, Pages 144-151, ISSN 0927-7765, http://dx.doi.org/10.1016/j.colsurfb.2016.04.052.

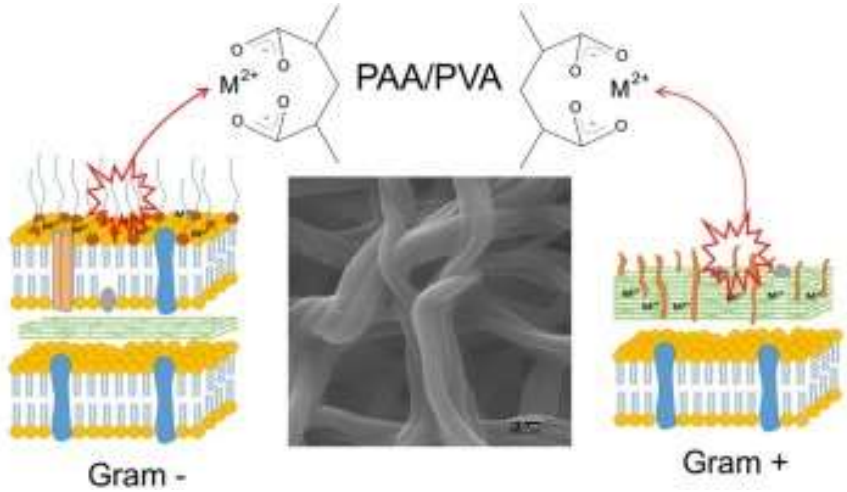

http://www.sciencedirect.com/science/article/pii/S0927776516303216

Antimicrobial activity of poly(vinyl alcohol)-poly(acrylic acid) electrospun nanofibers

Javier Santiago-Morales[1], Georgiana Amariei[1], 1, Pedro Letón[1,2], Roberto Rosal[1,2,*]

[1] Department of Chemical Engineering, University of Alcalá, E-28871 Alcalá de Henares, Madrid, Spain
[2] Madrid Institute for Advanced Studies of Water (IMDEA Agua), Parque Científico Tecnológico, E-28805, Alcalá de Henares, Madrid, Spain

* Corresponding author: roberto.rosal@uah.es

Abstract

Electrospun nanofibers were prepared from blends of poly(acrylic acid) (PAA) and poly(vinyl alcohol) (PVA). The fibers were stabilized by heat curing at 140 °C via anhydride and ketone formation and crosslinking esterification. The antimicrobial effect was assessed using strains of *Escherichia coli* and *Staphylococcus aureus* by tracking their capacity to form colonies and their metabolic impairment upon contact with PAA/PVA membranes. Membranes containing > 35 wt. % PAA displayed significant antibacterial activity, which was particularly high for the gram-positive S. . aureus. All membranes were negatively charged, with surface ζ-potential in the (-34.5)−(-45.6) mV range, but the electrostatic interaction with the negatively charged cells was not the reason for the antimicrobial effect. Neither pH reduction nor the passing of non-crosslinked polymers to the solution affected microbial growth. The antibacterial activity was attributed to the chelation of the divalent cations stabilizing the outer cell membrane. The effect on gram-positive bacteria was attributed to the destabilization of the peptidoglycan layer. The sequestration of divalent cations was demonstrated with experiments in which calcium and a chelating agent were added to the cultures in contact with membranes. The damage to bacterial cells was tracked by measuring their surface charge and the evolution of intracellular calcium during the early stages after contact with PAA/PVA membranes.

Keywords: Glass-like carbon films, reversible wettability, ultraviolet irradiation; bacterial colonisation; surface hydrophilicity

1. Introduction

Pressure-driven membrane processes are widely used separation tools for water and wastewater treatment and for different separations in many industries. Membrane biofouling, which is due to the microbial growth and biofilm formation on membrane surface, is a major problem encountered in membrane filtration processes. Biofouling reduces membrane permeability and membrane service life and rises operating costs [1]. Many strategies have been developed to prepare biofouling resistant materials based on surface modification in an attempt to control surface features such as hydrophilicity, charge or roughness [2-4]. Other approaches used biocidal nanomaterials groups [5, 6].

Poly(acrylic acid) (PAA) is a ionizable hydrophilic polymer used for drug release [7], pH and gas sensing [8, 9] and surface hydrophilicity enhancement [10-11]. PAA forms hydrogels with a swelling behavior depending on its easily ionizable carboxyl groups, the pKa of which is 4.5 [12]. Its antimicrobial activity has been recently reported for PAA block copolymers with poly(styrene) and poly(methyl methacrylate) containing more than 40 wt.% of PAA and has been attributed to the pH drop due to the dissociation of carboxylic groups that impairs pH homeostasis and eventually leads to the damage of proteins, membranes and DNA [13]. The same group has studied the antimicrobial effect of poly(styrene)-poly(acrylic acid)-diblock copolymers and suggested that the acidic conditions created by the dissociation of carboxylic groups were related to their antimicrobial activity. The bactericidal activity was attributed to an ion-exchange effect [14].

The water solubility of PAA can be overcome using short-wavelength ultraviolet (UVC) crosslinking under nitrogen atmosphere, although its effectiveness is limited by sample thickness [15]. The addition of hydroxyl-containing agents results in a transesterification that renders insoluble materials [16]. The curing of PAA with poly(vinyl alcohol) (PVA) has been frequently described [17-18]. PVA has been proposed for tissue engineering or other biomedical applications thanks to its material properties and excellent biocompatibility [19]. The crosslinking effectiveness and the swelling behavior of PAA/PVA fibers depend on several factors including annealing time and temperature, the molecular weight of polymers and their mixture ratio. PAA/PVA crosslinking has been shown more effective for high molecular weight polymers (> 250 kDa), higher temperature (>120 °C) and longer annealing times, although an excess in any of them results in polymer degradation [20].

Electrospinning is a simple and potentially scalable method for the preparation of nanofibers [21]. It involves the application of an electrical field to overcome the surface tension threshold of a dissolved or melt polymer. A thin jet of charged polymer draws out from the tip of a droplet reaching a terminal velocity and whipping into a fast moving spiral until being recovered on a collector usually as a non-woven mat [22]. Electrospun fibers have been widely used in several fields including biomedical applications (scaffolds for tissue engineering, drug delivery, medical implants, biosensors and wound dressing) and water filtration [23]. The versatility of electrospun fibers arises from their remarkable properties, which include high pore interconnectivity, high surface area-to-volume ratio and easy surface functionalization [24-25]. Both PAA and PVA have been studied to produce polymer fibers in the nano- to a few micrometers range searching for a simple method of preparing large surface and highly tailored materials [26-28].

The aim of this work was to prepare electrospun nanofibers from blends of PAA and PVA in order to assess their antibacterial activity. The purpose was to combine the antimicrobial activity of PAA with the high specific surface of electrospun fibers in order to prepare membranes with potential application in water filtration or for the manufacture of general-purpose antibacterial tissues. The antimicrobial effect was assessed with strains of *Escherichia coli* and *Staphylococcus aureus* by tracking their ability to form colonies and their metabolic impairment. An insight into the mode of the antimicrobial action of PAA/PVA membranes is presented.

2. Materials and methods

2.1. Preparation of electrospun membranes

Poly(vinyl alcohol) (PVA, 89–98 kDa, 99 +% hydrolyzed) and poly(acrylic acid) (PAA, 450 kDa) were provided by Sigma-Aldrich. Ultrapure water was obtained from a Millipore Milli-Q System with a resistivity of at least 18 MΩ cm. The electrospinning solution was prepared by mixing different amounts of 8 wt.% PAA and 15 wt.% PVA solutions in water. To dissolve PVA, the solution was heated at 90 °C under reflux until complete dissolution. PAA and PVA solutions were further stirred for 24 h at room temperature. To prepare the final electrospinning solutions (listed with their properties in Table S1, Supplementary Material), the required amount of 8 wt.% PAA solution and water were added dropwise to the 15 wt.% PVA solution and stirred for 2 h at room temperature. Prior to electrospinning, the solution was degassed. The conductivity of the electrospinning solution was measured using a Crison conductimeter. Surface tension was determined using a K6 Krüss Tensiometer. Rheology parameters were determined with a Bohlin Visco 88 viscometer using DIN 53019 coaxial cylinders at 25 ± 0.2 °C. The viscosity of polymeric solutions was obtained at a shear rate of 100 ± 1 s^{-1}. Consistency indexes and power law exponents were calculated from the Ostwald–de Waele relationship using shear rates in the 25 to 800 s−1 range. All solutions behaved as a shear-thinning fluid, with law exponent < 1 (Table S1).

The electrospinning solution was placed in a 5 mL syringe with a 23-gauge stainless steel blunt-tip needle. A positively charged DC high voltage power source (Glassman FJ Series, High Bridge, NJ) was connected to the needle tip. The negatively charged electrode was connected to a drum collector (PDrC-3000, Yflow, Spain) rotating at 100 min^{-1}. The applied voltage was 23 kV and the distance between needle tip and collector was 23 cm. The flowrate was set up at 0.8 mL/h using a syringe pump (PHD 2000, Harvard, Holliston, MA). The nanofibers were prepared at 25 °C and ∼40% relative humidity. The electrospun fibers recovered from the collector were dried at 50 °C for 24 h and then cured at 140 °C for 30, 60 and 120 min to yield crosslinked membranes.

2.2. Membrane characterization

The surface morphology of PAA/PVA membranes was assessed using a field emission Scanning Electron Microscope (SEM) DSM-950 (Zeiss, Oberkochen, Germany) operating at 25 kV on gold sputter-coated samples. Attenuated Total Reflectance Fourier Transform Infrared (ATR-FTIR) spectra were obtained in the 4000–650 cm^{-1} range using a Thermo-Scientific Nicolet iS10 apparatus with a Smart iTR-Diamond ATR module. The crosslinking of PAA/PVA nanofibers and their stability was assessed by immersion in deionized water. Accurately weighed pieces of dry electrospun membranes were crosslinked, weighed again and immersed in water to remove any material that may have not crosslinked. The NPOC (Non-Purgeable Organic Carbon) and UV absorbance at 220 nm of the resulting solutions were analysed using a Total Organic Carbon (TOC) analyzer (Shimadzu, TOC-VCSH) and a Shimadzu UV-1800 spectrophotometer, respectively. Water uptake was measured using dried membranes immersed in distilled water at 25 °C for 24 h. The membranes were then drained and weighed again, water uptake being expressed as percentage of weight gain relative to dry membranes.

The ion exchange capacity (IEC) of crosslinked membranes was determined by titrating carboxyl groups. Dried membrane samples were accurately weighed and converted to the protonated form using 0.1 M HCl during 24 h. The protonated specimens were washed with deionized water to remove the excess of HCl and immersed in 0.1 M NaOH for 24 h. The resulting NaOH solution was titrated with 0.1 M HCl. IEC was expressed as moles of carboxyl groups per unit mass of dry membrane. The experiments were carried out under nitrogen atmosphere.

Surface ζ-potential measurements of PAA/PVA membranes were performed using dynamic light scattering in a Zetasizer Nano-ZS apparatus equipped with the ZEN 1020 Surface Zeta Potential (Malvern Instruments Ltd., UK). A section of the membrane with the prescribed dimensions was glued to the sample holder using Araldite adhesive. The sample was inserted in a disposable plastic 10 mm square cuvette containing 10 mM KCl, pH 7.0, aqueous solution with of 0.5 wt.% PAA (450 kDa) as tracer (a negatively-charged tracer is required for negatively-charged surfaces). Measurements were conducted at 25 °C at six different distances from sample surface in order to calculate surface ζ-potential.

2.3. Microbiological assays

The gram-negative *E. coli* (CETC 516) and the gram-positive *S. aureus* (CETC 240) bacteria were used as reference strains for antibacterial testing. The microorganisms were preserved at −80 °C in glycerol (20% v/v) until use. Reactivation was performed in nutrient broth (NB, 10 g L^{-1} peptone, 5 g L^{-1} sodium chloride, 5 g L^{-1} meat extract and, for solid media, 15 g L^{-1} powder agar, pH 7.0 ± 0.1). All the chemicals used for culture media were microbiological grade obtained from Conda (Spain). The microbiological assays were performed using vacuum-dried specimens placed into the wells of sterile 24-well plates. Bacterial suspensions with a concentration of approximately 10^6 Colony Forming Units (CFU) mL^{-1} were pipetted into each well (0.4 mL per mg membrane, cut in pieces of 8 × 8 mm. approx.) and incubated at 36 ± 1 °C for 20 h. After exposure, the membranes were transferred to 24-well plates containing each well 2 mL phosphate buffer saline (PBS) and orbitally shaken at 5 °C for 15 min in order to remove non-adhered cells. The cells detached from membrane surface were recuperated using 2 mL/well SCDLP broth (Soybean casein digest broth with lecithin and polyoxyethylene sorbitan monooleate) followed by 30 min shaking according to the prescription of ISO 22196. The cells from the supernatant liquid in contact with membranes and the cells removed from their surface were evaluated by plate count. Briefly, aliquots of both liquids were placed in sterile 96 well microtiter plates in 10-fold serial dilutions in PBS. Replicated 10 μL spots were plated on Petri dishes containing NB agar-medium as described above. After 24 h incubation at 36 ± 1 °C, CFU were counted using a CL-1110 counting instrument (Acequilabs, Spain). For colony number estimations, at least three replicates of at least two serial dilutions were considered.

Bacterial viability was also tested using fluorescein diacetate (FDA), a non-fluorescent compound, which is transformed by active esterases in fully functional cells to yield the green fluorescent compound fluorescein. The liquid fraction in contact with membranes was analyzed in 96-well microplates by adding 195 μL of bacterial suspension and 5 μL of FDA (0.02% w/w in dimethyl sulfoxide, DMSO) to each well. Then the plate was incubated at 25 °C for 5 min after which, readings were performed every 5 minutes for 30 min (excitation, 485 nm; emission, 528 nm) using a fluorimeter (ThermoScientific™ FL, Ascent).

Bacterial surface charge was measured as ζ-potential in the same Zetasizer Nano-ZS apparatus mentioned before. The measurements were performed for at least two independent replicates with cells incubated at 36 °C in PBS with and without contact with PAA/PVA membranes.

Intracellular calcium was tracked using Fura-2 am (Invitrogen, ThermoFisher, Waltham, MA, USA). Fura-2 am is a fluorescent calcium probe internalized as acetoxymethyl, which is cleaved to the active form by intracellular esterases. Individual 1 mM Fura-2 am and 20% Pluronic F-127 stock solution were prepared in DMSO. Prior to the analyses, a fresh solution of 40 μM of Fura-2 am and Pluronic in PBS was prepared, 5 μL of which were added to 195 μL of the liquid containing bacteria in order to achieve 1 μM of Fura 2-am and incubated 10 min at 20 °C. Upon calcium binding, the fluorescent excitation maximum of the indicator shifts from 380 nm (calcium-free) to 340 nm (calcium-saturated). The ratio 340/380 was used as it depends only on calcium concentration and is independent on that of the probe.

3. Results and discussion

3.1. Preparation and characterization of membranes

Electrospun membranes prepared using the PAA/PVA weight ratios shown in Table S1 and stabilized by thermal crosslinking at 140 °C. Fig. 1 displays SEM micrographs of 83/17 PAA/PVA membranes as produced, after crosslinking (30 min) and after water immersion for several days until ensuring constant weight (and subsequent drying for SEM). The average diameter of 83/17 fibers as produced by electrospinning was 221 ± 45 nm (Fig. S1). The fiber diameter slightly increased with the proportion of PVA, with values of 290 ± 61 nm, 340 ± 83 nm and 309 ± 87 nm for 55/45, 35/65 and 19/81 PAA/PVA, respectively. This increase was a consequence of the viscosity increase and the conductivity decrease of polymer solutions with decreasing PAA ratio [18, 20]. After water immersion, the membranes kept their fiber-based morphology eventually merging at their contact points, which resulted in a uniform porous structure (Fig. 1). The transformation of a fibrous mat into a porous membrane due to water swelling has been reported elsewhere for PAA/PVA fibers [17, 18]. Fig. S1 shows detailed SEM micrographs of specimens prepared with different PAA/PVA ratios. A higher content of PAA resulted in lower water swelling (also shown as water uptake in Fig. S2) and a better preservation of the porous structure after water immersion.

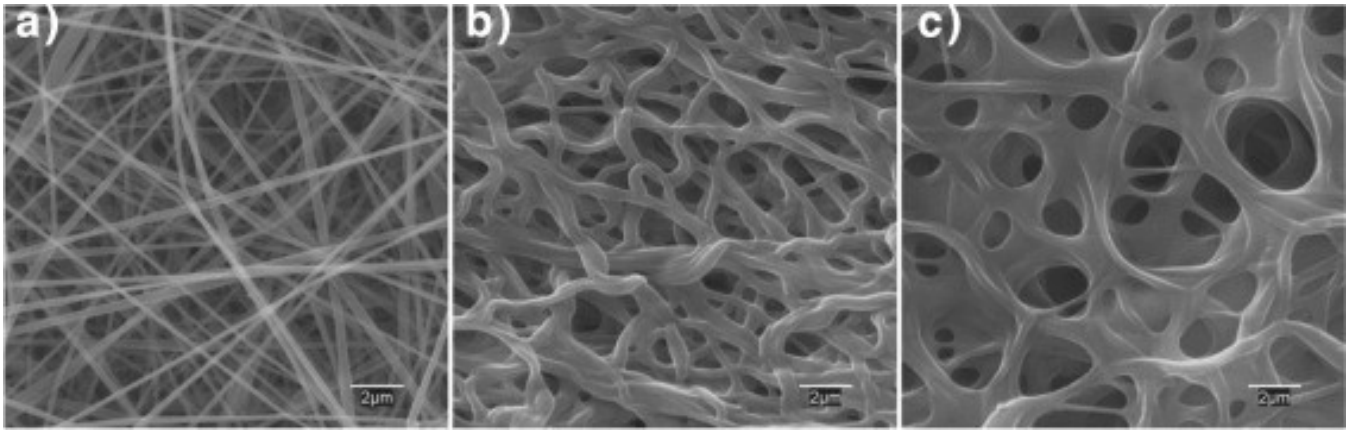

Figure 1. SEM micrographs of 83/17 PAA/PVA membranes freshly electrospun (a), after heat curing (b) and after water immersion until constant weight (c)

The ATR-FTIR spectra of electrospun membranes and their raw pure polymers are shown in Fig. S3a. The intensity of C=O stretching band at 1704 cm^{-1} agrees well with the relative amount of PAA in blends. The band at 3282 cm^{-1} corresponds to O-H stretching and decreased with PVA content, eventually overlapping with the broad COOH band at 2400–3400 cm^{-1}, which corresponds to PAA. After thermal treatment, the OH and C=O stretching bands decreased with curing time due to the formation of anhydride, ketone and ester groups [18], [29, 30]. ATR-FTIR spectra of all membranes during curing is shown in Fig. S3b. These changes were accompanied by a weight loss that reached a maximum value of 10.7 wt.% for 120 min thermal treatment of 83/17 PAA/PVA membranes. The loss was attributed to the release of residual acrylic acid monomers and CO_2 evolution from anhydride decarboxylation [31].

An increase in PVA content led to a lower reduction of C=O intensity at 1704 cm^{-1}, which was < 1% for 35/65 membranes. Samples with high PVA content also displayed low weight loss upon heating. These findings could indicate that anhydride formation is not playing a significant role except for membranes with PAA in large excess. Fig. S3b4 also shows that C=O peak shifted to higher wavenumbers during curing. The bands at 1715 cm^{-1} and 1722 cm^{-1} are compatible with aliphatic ketone and unsaturated ester C=O stretches, respectively, with ketone groups probably arising from the oxidation of PVA hydroxyl groups accompanied by water loss [20]. The process of ketone formation would be favored by the low pH of the electrospinning solution, which limits the extent of esterification. The fact that OH band at 2400–3400 cm^{-1} did not increase with reaction time could be due to the formation of hydrogen bonds between two consecutive ketone groups due to keto–enol tautomerism. The formation of ester groups could be tracked by the band at 1142 cm^{-1}, which is clearly visible in Figs. S3b3 and S3b4 and corresponds to C-O-C stretching.

The surface ζ-potential of electrospun fibers, assessed using electrophoretic light scattering at pH 7.0, is shown in Table S2. All the values are in the −34.5-(45.6) mV range with no significant effect of curing time. ζ-potential was lower (more negative) as PAA content increased, but differences were not high. The negative surface charge was obviously due to the ionization of the carboxylic moieties in PAA remaining after thermal treatment: at pH 7.0, PAA was almost completely deprotonated (pK_a 4.5).

The stability of electrospun membranes was tested by measuring the release of non-crosslinked polymers in water. Fig. S4 represents the absorbance (285 nm, 2.5 mg membrane mL^{-1}) and NPOC of water in contact with membranes for 24 h and 48 h. The results showed that the higher PVA content and the shorter crosslinking time, the higher the release of soluble organic matter. The maximum crosslinking efficiency led to a release of only 1.4 mg NPOC/g of membrane for 83/17 PAA/PVA fibers after 120 min curing. The lowest, 69.0 mg NPOC/g of membrane was observed for 19/81 PAA/PVA membranes with 30 min curing time due to the lower extension of crosslinking in membranes with high amount of PVA. All tested specimens were dried at room temperature and immersed again in water for another 24 h. NPOC values after the second 24 h conditioning time were roughly one order of magnitude lower than that observed during the first 24 h. Electrospun membranes with 83/17 PAA/PVA released < 0.4 mg NPOC/g of membrane. All the membranes used for microbiological assays were preconditioned in water during 48 h in order to gain as much chemical stability as possible.

3.2. Antibacterial effect

The microbiological studies assessed the antibacterial effect of PAA/PVA membranes to *E. coli* and *S. aureus*. Fig. 2 displays the microbial growth inhibition measured in the culture media kept in contact with membranes and for cells detached with SCDLP from membrane surface. In both cases, the bacterial strains were cultured with fibers for 20 h at their optimal growth temperature of 36 °C. Fig. 2 shows that *S. aureus* was more impaired than *E. coli* upon exposure

to PAA/PVA fibers, with a two-order of magnitude reduction in the number of viable organisms detached from the membrane versus one-order of magnitude for *E. coli.* The difference was much higher for the liquid culture in contact with membranes, for which the reduction in the number of colonies of *S. aureus* was orders of magnitude higher than for *E. coli*. The differences between both strains were probably a consequence of the tendency of *S. aureus* to form cellular aggregates rather than a different response to surface hydrophilicity [32, 33]. The maximum relative differences were obtained for fibers with the highest PAA content, 83/17 PAA/PVA, with significant reductions in the number of viable cells for fibers with > 35 wt.% PAA. The amount of bacteria adhered to membrane surface also decreased for increasing PAA ratio with significant reductions for 83/17 fibers with respect to the rest, particularly for S. aureus. The higher variability for the colony counting of bacteria detached from membranes was most probably due to the experimental procedure and because of the lower amount of cells. Also to the different amount of carboxylic groups among specimens, but followed the same trend observed for culture media in contact with membranes.

The antimicrobial effect is also shown in Fig. S5, which compares SEM micrographs of 83/17 PAA/PVA and 35/65 PAA/PVA membranes after 20 h in contact with cultures of E. coli and S. aureus. 83/17 PAA/PVA fibers appeared free of bacteria, while 35/65 showed colonization. Occasionally, some E. coli bacteria seemed deformed, although the damage is difficult to assess using SEM. The damage was apparent and recorded by measuring FDA, which tracks the metabolic activity of cells in contact with fibers. The results are shown in Fig. 3. According to FDA data, bacterial viability was significantly impaired by membranes with high PAA content, the effect being considerably greater for *S. aureus* than for *E. coli*. FDA signals were lower for membranes with high PAA ratio, particularly for those cured for a longer time. The maximum inhibition values were about 99% for S. aureus, a lower reduction than that observed from colony counting probably related to the presence of viable but non-culturable (VBNC) bacteria, which are cells with metabolic activity but fail to replicate in plate count assays. The lower effect observed for E. coli was probably insufficient to produce VBNC cells.

The amount of carboxyl groups in PAA/PVA fibers was quantified by measuring IEC as indicated before. IEC dropped from 13–17 mmol/g for 83/17 membranes to less than half for 19/81 PAA/PVA fibers (Fig. S2). This data suggest that the toxic effect could be related to the presence of acidic functional groups. It has been previously suggested that pH reduction due to PAA

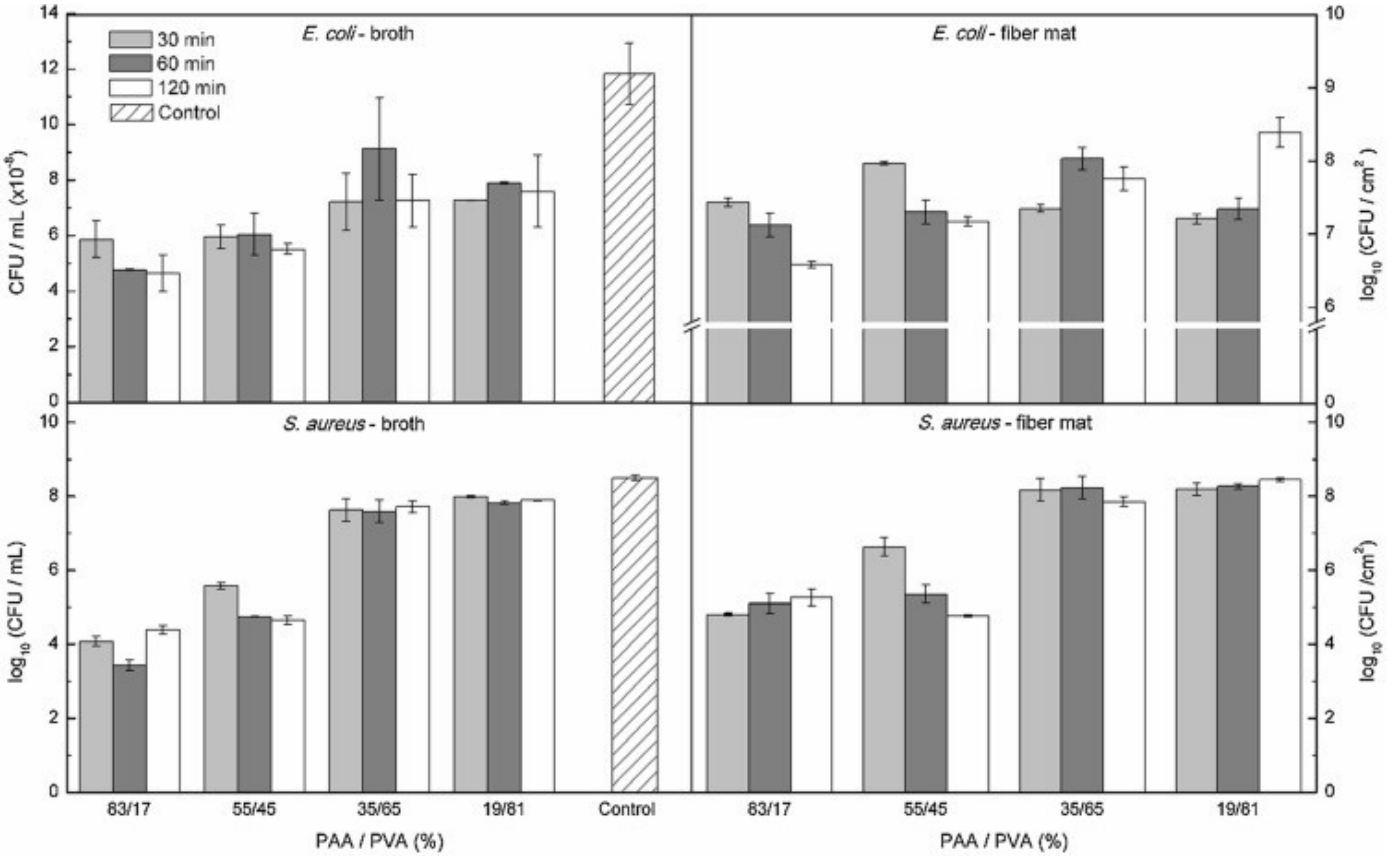

Figure 2. E Colony-forming units (CFU) in liquid media in contact with fibers (left) and for microorganisms detached from membranes (right). The data correspond to fibers with different PAA/PVA compositions and different curing time. The control was NB and cultures were kept in contact with bacteria for 20 h at 36 °C.

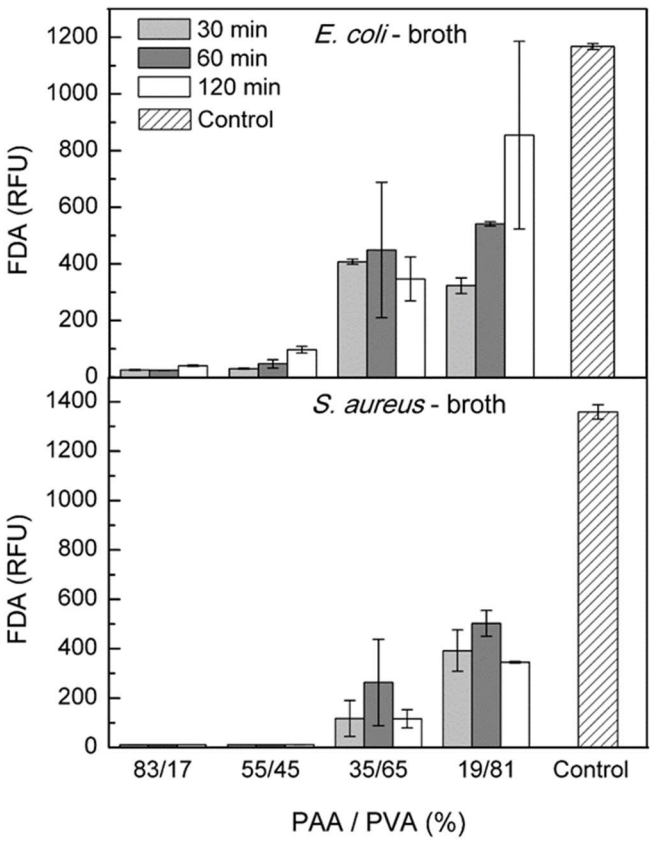

Figure. 3. FDA in Relative Fluorescence Units (RFU) for bacteria kept 20 h in contact with fibers prepared with different polymer composition and curing time.

dissociation could cause cell stress by disrupting cytoplasmic pH homeostasis. This would create a hostile microenvironment for bacteria preventing biofilm formation on PAA containing diblock copolymers [13]. In order to verify the role of pH, we performed experiments with carefully controlled pH at 7.0 and 5.5 (± 0.1). In order to avoid pH drift, 83/17 PAA/PVA membranes were preconditioned in NB medium for 2 hours. The microbial growth relative to controls (NB) is displayed in Fig. 4. The controls for both microorganisms grew at higher rate at pH 7.0, which is near the optimum for both bacteria (6-7 for *E. coli* and 7-7.5 for *S. aureus*). The contact with membranes resulted in a similar growth reduction irrespective of pH for both microorganisms, which amounted up to 99.9% reduction for *S. aureus*. These results indicate that pH cannot be considered as the determining factor for the antimicrobial effect observed.

During membrane preconditioning by immersion in water, a certain amount of non-crosslinked polymers dissolves as shown in Fig. S4. NPOC measurements showed that the amount of organic carbon released for 83/17 membranes was below 1 mg/g of membrane, which represents < 0.2 wt.% of the whole membrane and a total concentration in culture media lower than 0.8 mg L^{-1}, irrespective on whether the compound liberated was PVA or PAA. The toxicity of PAA and PVA on E. coli and S. aureus was tested to discard any biocidal effect due to the release of non-crosslinked PAA or PVA. The tests were conducted at concentrations reaching 1000 mg L^{-1} and the corresponding results are listed in Tables S3a and S3b. No significant toxicity was observed for PVA, while PAA led to a significant reduction of microbial growth (> 10%) only at concentrations near or over 100 mg L^{-1} for both microorganisms. For lower concentrations, in the 0.1–10 mg L^{-1} range, a certain growth stimulation was detected rather than inhibition. The release of residual non-crosslinked polymers could not to be behind the antimicrobial behavior of PAA/PVA membranes.

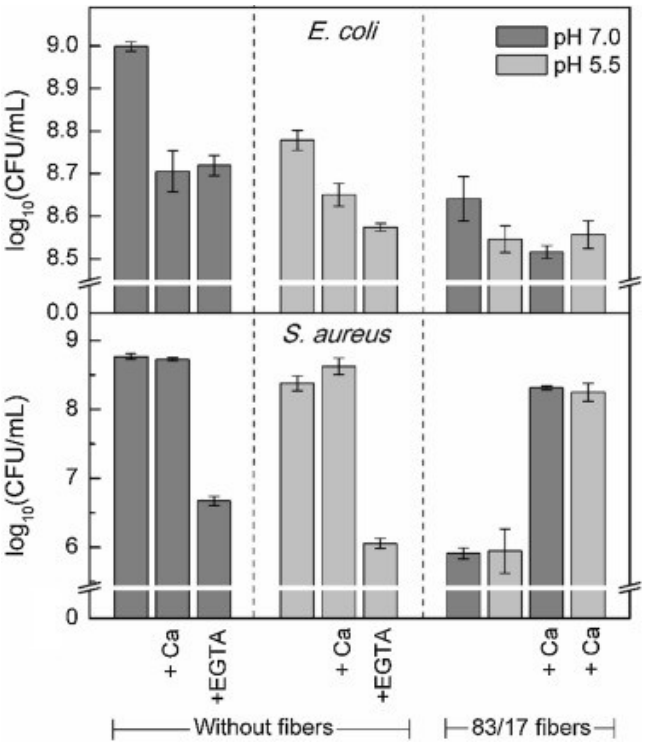

Figure 4. Effects on microbial growth of different culture conditions (pH 7.0 or 5.5; calcium and EGTA addition) for bacteria grown with or without contact with 83/17 fibers. The effect is shown as reduction of CFU/mL with respect to NB control.

Another factor usually claimed to explain the antimicrobial effect of charged surfaces is the electrostatic interaction between membrane and biofoulants [34]. Although there is some controversy, it is generally accepted that negatively charged surfaces are less prone to bio-adhesion than neutral surfaces [35]. A negative surface reduces biofouling because bacterial surfaces are also negatively charged at neutral pH. Table S2 lists surface potential for the membranes prepared in this work. The 83/17 PAA/PVA membrane displayed a surface zeta potential of −44.5 ± 7.6 mV (at pH 7), which arises from deprotonated carboxyl groups and would lead to a repulsive effect on bacterial cell walls. However, surface zeta potential was also negative and similar in value for other fiber compositions with considerably lower antimicrobial

effect, such as 35/65 and 19/81 formulations. These results point towards a negligible role of electrostatic forces to explain the antibacterial effect observed.

The chelation of divalent cations has been identified as a factor responsible for membrane destabilization affecting its permeability and eventually compromising cell viability [36]. It was shown that PAA behaves as a calcium chelator with a binding constant of $10^{5.3}$[37]. Besides, it is interesting to note that calcium binding to PAA occurs spontaneously due to an increase in entropy and not to electrostatic forces [38, 39]. The binding constant of calcium to the cell wall of *Bacillus subtilis* was $10^{4.6}$, meaning that PAA can remove calcium from the cell wall forming Ca-PAA complexes [40]. Thomas et al. studied the binding affinity of calcium for peptidoglycan with and without covalent binding to teichoic acid, which are the components of cell walls in gram-positive bacteria [41]. They obtained that the binding constants for high and low ratio of bound/unbound calcium were $10^{4.9}$ and 10^{6} respectively. Therefore, calcium can also be withdrawn from gram-positive bacterial envelopes except for high bound/unbound ratios. Grattzl et al., also pointed at the ion-exchange capacity of PAA to explain the antimicrobial effect of poly(acrylic acid) block copolymers and suggested that PAA-containing copolymers attract divalent counter-ions that balance the negative charges of the bacterial cell membrane components resulting in collapse of the cell membrane [14].

In order to check the get a deeper insight on the role of divalent metal chelation as a driver for the antimicrobial effect, a series of runs was undertaken in the presence of 15.5 mM EGTA (Ethylene Glycol Tetraacetic Acid). EGTA, a specific calcium chelator with binding constant of $10^{10.48}$[42], was combined with $CaCl_2$, 15.5 mM, as a chelatant neutralizer. The concentration of $CaCl_2$ was chosen to balance the total amount of carboxyl groups in the 30 min heat-cured 83/17 PAA/PVA fibers. The results are shown in Fig. 4 for *E. coli* and *S. aureus* grown in different conditions with and without calcium or EGTA in contact with 83/17 PAA/PVA fibers. The addition of calcium or EGTA to the culture medium reduced the growth of *E. coli* at both pH 5.5 and 7.0. The growth reduction for high calcium concentration can be associated to a decrease in ATPase activity [43]. A decrease in the growth rate of E. coli with evidence of enucleated cells followed the addition of 5 mM EGTA and was attributed to the destabilization of the outer membrane (OM) of gram-negative bacteria [44, 45]. The presence of calcium did not to affect the growth of *S. aureus* irrespective of pH, but EGTA reduced it two orders of magnitude. This strong chelating effect was almost completely neutralized by $CaCl_2$ addition as shown in Fig. 4.

The different behavior observed between E. coli and S. aureus can be rationalized in view of their cell wall structures. In E. coli, lipopolysaccharides (LPS) are a major part of the outer leaflet of the OM, which is a lipid bilayer that contains membrane proteins and is responsible for creating a negatively charged surface [46]. LPS consist of three regions: O-side chains, a saccharide core and lipid A. The two latter have anionic phosphate groups electrostatically balanced with divalent cations (Mg^{2+}, Ca^{2+}), which give stability to the assembly [47]. The removal of calcium from OM by PAA or other chelators results in a loss of the bilayer asymmetry and membrane integrity by destroying the interlocking of LPS molecules between the outer and inner leaflets. S. aureus, being a gram-positive bacterium, has no OM but a thick layer of peptidoglycan containing teichoic acids and proteins [48]. The carboxyl groups of proteins and peptidoglycan and the phosphate groups of teichoic acids provide gram-positive bacteria with a negatively charged surface that binds cationic counterions, which determine cell wall porosity and rigidity and, eventually, membrane integrity [49]. It was shown that Ca^{2+} displays higher affinity than the rest of divalent and monovalent cations for the cell walls of gram-positive bacteria [50]. Later, it was shown that calcium binds preferably to phosphate groups rather than carboxylic groups, although there is some controversy on the exact role played by both binding sites [41, 50]. Calcium bound to teichoic acids also plays an important role in calcium homeostasis and is a structure-determining ion for gram-positive bacteria [51].

The data support the hypothesis that calcium bound to the cell wall of both *E. coli* and *S. aureus* was withdrawn by PAA/PVA fibers. In the case of the gram-positive *S. aureus*, the effect on microbial growth was about two orders of magnitude higher than for the gram-negative *E. coli*. The most probable reason is that, while *E. coli* is protected by the outer membrane, the disruption of *S. aureus* peptidoglycan layer strongly compromises cell viability. This hypothesis is supported by the fact that the addition of calcium to 83/17 PAA/PVA membranes strongly reduced its antimicrobial effect, as shown in Fig. 4.

The effect of PAA/PVA membranes on bacteria can also be tracked by measuring bacterial ζ-potential. Fig. 5 (and Fig. S6 for *E. coli*) shows the evolution of the surface charge of *S. aureus* during 120 min after contact with PAA/PVA membranes. The initial surface charge was more negative for *S. aureus* (-6.4 ±0.8 mV) than for *E. coli* (-4.6 ± 0.6 mV). Thereafter, cultures exposed to PAA/PVA showed an increase of ζ-potential during the first 30 min and a reduction in the number of viable cells (Fig. 5, squares), while control cultures in PBS drifted towards more negative ζ-potential values and kept CFU constant (Fig. 5, triangles). A similar result was reported for S. aureus and *E. coli* in contact with an antimicrobial protein and was considered a consequence of the electrical depolarization of the bacterial membrane [48]. It has also been suggested that

cells in contact with highly negatively charged fibers may experience a medium with higher ionic strength, which is known to induce cell aggregation due to the reduction of the electrical double layer [52]. In order to prove the stress suffered by bacteria contacting PAA/PVA membranes, we tracked the changes in intracellular calcium as indicated before. Fig. 5 also plots the content of intracellular calcium relative to the value prior to exposure for *S. aureus* (Fig. S6 plots the same for *E. coli*). During the first minutes after contacting PAA/PVA fibers, the signal for intracellular calcium significantly decreased to recover thereafter.

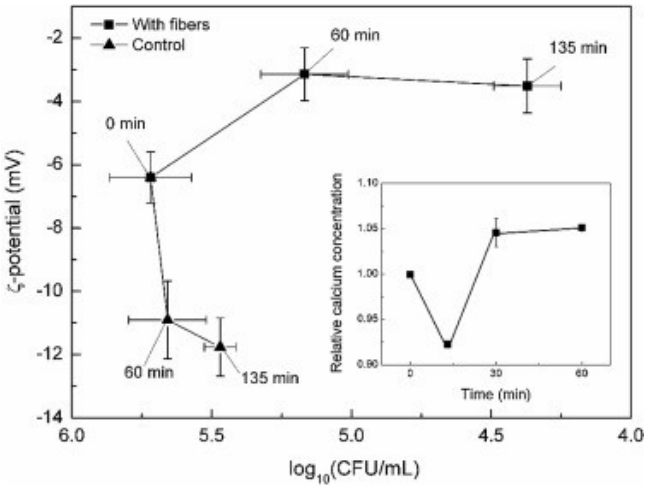

Figure 5. Changes in ζ-potential of bacteria and colony-forming units (CFU) for *S. aureus* exposed to 83/13 PAA/PVA 30 min mat in PBS (■). Control culture in PBS without fibers shown for reference (▲). The inset displays the variation of relative content of intracellular calcium for *S. aureus* exposed to fibre mat in PBS.

This result could be explained by the loss of Ca^{2+} by PAA, and the subsequent attempt to restore calcium equilibrium. Intracellular calcium is an essential intermediate in stimulus–response phenomena, tightly regulated in prokaryotic cells and transients in calcium concentration have been shown to take place in response to a number of environmental stresses [53, 54].

4. Conclusions

In this work, we studied the antimicrobial activity of electrospun nanofibers prepared form blends of poly(acrylic acid) and poly(vinyl alcohol). The fibers formed membranes stabilized via thermal crosslinking esterification. The growth of the bacteria *S. aureus* and *E. coli* was significantly impaired by PAA/PVA membranes containing > 35 wt. % PAA. PAA/PVA membranes were negatively charged, but we showed that the electrostatic repulsion of bacterial cell envelopes was not related to their antimicrobial effect. Neither pH reduction nor the solubilization of non-crosslinked PAA or PVA created a bactericidal environment. The binding of the divalent cations that stabilize prokaryotic membranes was identified as the cause for metabolic impairment and growth reduction. The damage was confirmed by measuring bacterial surface charge and the evolution of intracellular calcium after cell contact with PAA/PVA membranes.

Acknowledgements

Financial support for this work was provided by the FP7-ERA-Net Susfood, 2014/00153/001, the Spanish Ministry of Economy and Competitiveness, CTM2013-45775 and the Dirección General de Universidades e Investigación de la Comunidad de Madrid, Research Network S2013/MAE-2716. Two of the authors, JSM and GA, thanks the University of Alcalá for the award of post-doctoral and pre-doctoral grants, respectively.

References

1 W. Guo, H.H. Ngo and J. Li, A mini-review on membrane fouling, Biores. Technol. 122 (2012) 27-34; doi:10.1016/j.biortech.2012.04.089.

2 V. Kochkodan, D.J. Johnson and N. Hilal, Polymeric membranes: Surface modification for minimizing (bio)colloidal fouling, Adv. Colloid Interface Sci. 206 (2014) 116-140; doi:10.1016/j.cis.2013.05.005.

3 J. Yin and B. Deng, Polymer-matrix nanocomposite membranes for water treatment, J. Memb. Sci. 479 (2015) 256-275; doi:10.1016/j.memsci.2014.11.019.

4 M.R. El-Aassar, M.M.G. Fouda and E.R. Kenawy, Electrospinning of functionalized copolymer nanofibers from poly(acrylonitrile-co-methyl methacrylate), Adv. Polym. Technol. 32 (213) 1-11; doi: 10.1002/adv.21329.

5 A. Dasari, J. Quirós, B. Herrero, K. Boltes, E. García-Calvo and R. Rosal, Antifouling membranes prepared by electrospinning polylactic acid containing biocidal nanoparticles, J. Memb. Sci. 405-406 (2012) 134-140; doi: 10.1016/j.memsci.2012.02.060.

6 M.M.G. Fouda, M.R. El-Aassar and S.S. Al-Deyab, Antimicrobial activity of carboxymethyl chitosan/polyethylene oxide nanofibers embedded silver nanoparticles, Carbohyd. Polym. 92 (2013) 1012–1017; doi: 10.1016/j.carbpol.2012.10.047.

7 P. Gupta, K. Vermani and S. Garg, Hydrogels: from controlled release to pH-responsive drug delivery, Drug Discovery Today 7 (2002) 569-579; doi:10.1016/S1359-6446(02)02255-9.

8 P. Hu, X. Dong, W.C. Wong, L.H. Chen, K. Ni and C.C. Chan, Photonic crystal fiber interferometric pH sensor based on polyvinyl alcohol/polyacrylic acid hydrogel coating, Applied Optics 54 (2015) 2647-2652; doi: 10.1364/AO.54.002647.

9 B. Ding, M. Yamazaki and S. Shiratori, Electrospun fibrous polyacrylic acid membrane-based gas sensors, Sens. Actuators B 106 (2005) 477-483; doi:10.1016/j.snb.2004.09.010.

10 M.S. Rahaman, H. Thérien-Aubin, M. Ben-Sasson, C.K. Ober, M. Nielsen, and M. Elimelech, Control of biofouling on reverse osmosis polyamide membranes modified with biocidal nanoparticles and antifouling polymer brushes. J. Mater. Chem. B 2 (2014) 1724-1732; doi: 10.1039/C3TB21681K.

11 S. Zhou, A. Xue, Y. Zhao, M. Li, H. Wang and W. Xing, Grafting polyacrylic acid brushes onto zirconia membranes: Fouling reduction and easy-cleaning properties, Sep. Purif. Technol. 114 (2013) 53-63; doi:10.1016/j.seppur.2013.04.023.
12 J.E. Elliott, M. Macdonald, J. Nie and C.N. Bowman, Structure and swelling of poly(acrylic acid) hydrogels: effect of pH, ionic strength, and dilution on the crosslinked polymer structure, Polymer 45 (2004) 1503-1510; doi:10.1016/j.polymer.2003.12.040.
13 G. Gratzl, C. Paulik, S. Hild, J.P. Guggenbichler and M. Lackner, Antimicrobial activity of poly(acrylic acid) block copolymers, Mater. Sci. Eng. C 28 (2014) 94-100; doi:10.1016/j.msec.2014.01.050.
14 G. Gratzl, S. Walkner, S. Hild, A.W. Hassel, H.K. Weber and C. Paulik, Mechanistic approaches on the antibacterial activity of poly(acrylic acid) copolymers, Colloids Surf. B Biointerfaces 126 (2015) 98–105; doi: 10.1016/j.colsurfb.2014.12.016.
15 A. Gestos, P.G. Whitten, G.M. Spinks and G.G. Wallace, Crosslinking neat ultrathin films and nanofibres of pH-responsive poly(acrylic acid) by UV radiation, Soft Matter 6 (2010) 1045-1052; doi: 10.1039/B923831J.
16 L. Li and Y.L. Hsieh, Ultra-fine polyelectrolyte fibers from electrospinning of poly(acrylic acid), Polymer 46 (2005) 5133-5139; doi:10.1016/j.polymer.2005.04.039.
17 J.C. Park, T. Ito, K.O. Kim, K.W. Kim, B.S. Kim, M.S. Khil, H.Y. Kim and I.S. Kim, Electrospun poly(vinyl alcohol) nanofibers: effects of degree of hydrolysis and enhanced water stability, Polym. J. 42 (2010) 273-276; doi:10.1038/pj.2009.340.
18 X. Jin and Y.L. Hsieh, pH-responsive swelling behavior of poly (vinyl alcohol)/poly (acrylic acid) bi-component fibrous hydrogel membranes, Polymer 46 (2005) 5149-5160; doi:10.1016/j.polymer.2005.04.066.
19 P. Supaphol and S. Chuangchote, On the electrospinning of poly (vinyl alcohol) nanofiber mats: a revisit, J. Appl. Polym. Sci. 108 (2008) 969-978; doi: 10.1002/app.27664.
20 K. Kumeta, I. Nagashima and S. Matsui, K. Mizoguchi, Crosslinking reaction of poly (vinyl alcohol) with poly(acrylic acid) (PAA) by heat treatment: effect of neutralization of PAA, J. Appl. Polym. Sci. 90 (2003) 2420-2427; doi: 10.1002/app.12910.
21 N. Bhardwaj and S.C. Kundu, Electrospinning: a fascinating fiber fabrication technique, Biotechnol. Adv. 28 (2010) 325-347; doi:10.1016/j.biotechadv.2010.01.004.
22 P.K. Bhattacharjee and G.C. Rutledge, Electrospinning and polymer nanofibers: process fundamentals, in: P. Ducheyne, K.E. Healy, D.W. Hutmacher, D.W. Grainger, C.J. Kirkpatrick (Eds.), Comprehensive Biomaterials, Elsevier Science, Amsterdam, 2011, 497-512.
23 J. Quirós, K. Boltes and R. Rosal, Bioactive applications for electrospun fibers, Polym. Rev., pre-published online; doi: 10.1080/15583724.2015.1136641.
24 F.E. Ahmed, B.S. Lalia and R. Hashaikeh, A review on electrospinning for membrane fabrication: Challenges and applications, Desalination 356 (2015) 15-30; doi:10.1016/j.desal.2014.09.033.
25 L. Weng and J. Xie, Smart electrospun nanofibers for controlled drug release: Recent advances and new perspectives, Curr. Pharm. Des. 21 (2015) 1944-1959; doi: 10.2174/1381612821666150302151959.
26 R.H.F. Zômpero, A. López-Rubio, S.C. Pinho, J.M. Lagarón and L.G. Torre, Hybrid encapsulation structures based on β-carotene-loaded nanoliposomes within electrospun fibers, Colloids Surf. B Biointerfaces 134 (2015) 475–482; doi:10.1016/j.colsurfb.2015.03.015.
27 B. Chaudhuri, B. Mondal, S.K. Ray and S.C. Sarkar, A novel biocompatible conducting polyvinyl alcohol (PVA)-polyvinylpyrrolidone (PVP)-hydroxyapatite (HAP) composite scaffolds for probable biological application, Colloids Surf. B Biointerfaces, in press, doi:10.1016/j.colsurfb.2016.03.027.
28 B .Kim, H. Park, S.H Lee and W.M. Sigmund, Poly (acrylic acid) nanofibers by electrospinning, Mater. Lett. 59 (2005) 829-832; doi: 10.1016/j.matlet.2004.11.032.
29 K. Arndt, A. Richter, S. Ludwig, J. Zimmermann, J. Kressler, D. Kuckling and H. Adler, Poly(vinyl alcohol)/poly (acrylic acid) hydrogels: FT-IR spectroscopic characterization of crosslinking reaction and work at transition point, Acta Polym. 50 (1999) 383-390; doi: 10.1002/(SICI)1521-4044(19991201)50:11/123.3.CO;2-Q.
30 P. Thomas, J.P. Guerbois, G. Russell and B. Briscoe, FTIR study of the thermal degradation of poly (vinyl alcohol), J. Therm. Anal. Calorim. 64 (2001) 501-508; doi: 10.1023/A:1011578514047.
31 S. Dubinsky, G.S. Grader, G.E. Shter and M.S. Silverstein, Thermal degradation of poly (acrylic acid) containing copper nitrate, Polym. Degrad. Stab. 86 (2004) 171-178; doi:10.1016/j.polymdegradstab.2004.04.009.
32 J. Haaber, M.T. Cohn, D. Frees, T.J. Andersen, H. Ingmer H, Planktonic aggregates of *Staphylococcus aureus* protect against common antibiotics, PLoS ONE 7 (2012) e41075.
33 A.G. Karakeçili, M. Gümüşderelioglu, Comparison of bacterial and tissue cell initial adhesion on hydrophilic/hydrophobic biomaterials, J. Biomater. Sci., Polym. Ed., 13(2002) 185-196.
34 V. Kochkodan and N. Hilal, A comprehensive review on surface modified polymer membranes for biofouling mitigation, Desalination 356 (2015) 187-207; doi:10.1016/j.desal.2014.09.015.
35 J.D. Bryers, Biofilms and the technological implications of microbial cell adhesion, Colloids Surf. B: Biointerfaces 2 (1994) 9-23; doi: 10.1016/0927-7765(94)80013-8.
36 M. Vaara, Agents that increase the permeability of the outer membrane, Microbiol. Rev. 56 (1992) 395-411.
37 D. Changa, The binding of free calcium ions in aqueous solution using chelating agents, phosphates and poly(acrylic acid), J. Am. Oil Chem. Soc. 60 (1983) 618-622; doi: 10.1007/BF02679800.
38 C.G. Sinn, R. Dimova and M. Antonietti, Isothermal titration calorimetry of the polyelectrolyte/water interaction and binding of Ca2+: Effects determining the quality of polymeric scale inhibitors, Macromolecules 37 (2004) 3444–3450; doi: 10.1021/ma030550s.

39 P. Cañizares, A. Pérez, R. Camarillo, J. Llanos and M. López, Selective separation of Pb from hard water by a semi-continuous polymer-enhanced ultrafiltration process (PEUF), Desalination 206 (2007) 602-613; doi:10.1016/j.desal.2006.04.066.
40 R.J. Doyle, T.H. Matthews and U.N. Streips, Chemical basis for selectivity of metal ions by the *Bacillus subtilis* cell wall, J. Bacteriol. 143 (1980) 471-480.
41 K.J. Thomas and C.V. Rice, Revised model of calcium and magnesium binding to the bacterial cell wall, Biometals 27 (2014) 1361-1370; doi: 10.1007/s10534-014-9797-5.
42 S. Matsuda and Y. Koichi, The apparent binding constants of Ca^{2+} to EGTA and heavy meromyosin, J. Biochem. 88 (1980) 1515-1520.
43 D.J. Evans, Membrane adenosine triphosphatase of Escherichia coli: activation by calcium ion and inhibition by monovalent cations, J. Bacteriol. 100 (1969) 914-922.
44 M. Wachi, N. Iwai, A. Kunihisa and K. Nagai, Irregular nuclear localization and anucleate cell production in Escherichia coli induced by a Ca^{2+} chelator, EGTA, Biochimie 81 (1999) 909-913; doi:10.1016/S0300-9084(99)00204-7.
45 M. Herrmann, E. Schneck, T. Gutsmann, K. Brandenburg and M. Tanaka, Bacterial lipopolysaccharides form physically cross-linked, two-dimensional gels in the presence of divalent cations, Soft Matter 11 (2015) 6037-6044; doi: 10.1039/C5SM01002K.
46 T.J. Silhavy, D. Kahne and S. Walker, The bacterial cell envelope. Cold Spring Harb. Perspect. Biol. 2 (2010) a000414; doi: 10.1101/cshperspect.a000414.
47 L.A. Clifton, M.W. Skoda, A.P. Le Brun, F. Ciesielski, I. Kuzmenko, S.A. Holt and J.H. Lakey, Effect of divalent cation removal on the structure of gram-negative bacterial outer membrane models, Langmuir 31 (2014) 404-412; doi: 10.1021/la504407v.
48 M.M. Domingues, P.M. Silva, H.G. Franquelim, F.A. Carvalho, M.A. Castanho and N.C. Santos, Antimicrobial protein rBPI 21-induced surface changes on gram-negative and gram-positive bacteria, Nanomed. Nanotechnol. Biol. Med. 10 (2014) 543-551; doi:10.1016/j.nano.2013.11.002.
49 R.E. Marquis, K. Mayzel and E.L. Carstensen, Cation exchange in cell walls of gram-positive bacteria, Can. J. Microbiol. 22 (1976) 975-982.
50 R.K. Rose, S.P. Matthews and R.C. Hall, Investigation of calcium-binding sites on the surfaces of selected gram-positive oral organisms, Arch. Oral Biol. 42 (1997) 595-599; doi: 10.1016/S0003-9969(97)00062-9.
51 A.C. Plette, M.F. Benedetti and W.H. van Riemsdijk, Competitive binding of protons, calcium, cadmium, and zinc to isolated cell walls of a gram-positive soil bacterium. Environ. Sci. Technol. 1996, 30 (6), 1902-1910; doi: 10.1021/es950568l.
52 O. Habimana, A. Semião and E. Casey, The role of cell-surface interactions in bacterial initial adhesion and consequent biofilm formation on nanofiltration/reverse osmosis membranes, J Membrane Sci. 454 (2014) 82-96; doi:10.1016/j.memsci.2013.11.043.
53 D.C. Dominguez, Calcium signalling in bacteria, Mol. Microbiol. 54 (2004) 291-297; doi:10.1111/j.1365-2958.2004.04276.x.
54 I. Torrecilla, F. Leganés, I. Bonilla and F. Fernández-Piñas, Use of recombinant aequorin to study calcium homeostasis and monitor calcium transients in response to heat and cold shock in cyanobacteria, Plant Physiol. 123 (2000 , 123(1) 161-176; doi: 10.1104/pp.123.1.161.

Supplementary Material

Antimicrobial activity of poly(vinyl alcohol)-poly(acrylic acid) electrospun nanofibers

Javier Santiago-Morales[1], Georgiana Amariei[1], 1, Pedro Letón[1,2], Roberto Rosal[1,2,*]

[1] Department of Chemical Engineering, University of Alcalá, E-28871 Alcalá de Henares, Madrid, Spain
[2] Madrid Institute for Advanced Studies of Water (IMDEA Agua), Parque Científico Tecnológico, E-28805, Alcalá de Henares, Madrid, Spain

* Corresponding author: roberto.rosal@uah.es

The following is included as supplementary material:

Table S1. Properties of polymer solutions.

Table S2. Surface zeta potential of membranes.

Table S3a. Toxicity of PAA exposed to *S. aureus* and *E. coli*.

Table S3b. Toxicity of PVA exposed to *S. aureus* and *E. coli*.

Fig. S1. SEM micrographs and diameters of PAA/PVA fibers freshly electrospun (a), after heat-treating at 140ºC for 30 min (b), and after water immersion (c)

Fig. S2. Carboxylic acid groups on fibers and swelling behavior expressed as water uptake for different PAA/PVA ratio and curing times.

Fig. S3a. ATR- FTIR spectra of freshly electrospun PAA/PVA fibers and pure PAA and PVA.

Fig. S3b1. ATR- FTIR spectra of 83/17 PAA/PVA fibers for different curing time.

Fig. S3b2. ATR- FTIR spectra of 55/45 PAA/PVA fibers for different curing time.

Fig. S3b3. ATR- FTIR spectra of 35/65 PAA/PVA fibers for different curing time.

Fig. S3b4. ATR- FTIR spectra of 19/81 PAA/PVA fibers for different curing time.

Fig. S4. Polymer release measured as absorbance increase absorbance (a) and NPOC after the first (filled symbols, 24 h) and second water immersion (empty symbols, 24+24 h) for membranes prepared in different conditions.

Fig. S5. Fibers of 83/17 (A and C) and 35/65 (B and D) PA/PVA after being 20 h in contact with cultures of *S. aureus* (A and B) and *E. coli* (C and D).

Fig. S6. Colony-forming units (CFU, empty symbols), ζ-potential of bacteria (filled symbols) and relative content of intracellular calcium (○) for *E. coli* exposed to 83/13 PAA/PVA 30 min in PBS (■). Control culture in PBS without fibers shown as a reference (▲).

Colloids and Surfaces B Biointerfaces, 146, 144-151, 2016

Table S1. Properties of polymer solutions.

Membrane PAA/PVA (wt %)	PAA (wt %)	PVA (wt %)	pH	Conductivity (µS/cm)	Surface Tension (mN/m)	Viscosity (mPa · s) at 100 s^{-1}	Consistency Index (Pa · s^n)*	n*
83/17	5.7	1.2	2.4	1351	50	128 ± 1	0.211 ± 0.003	0.903 ± 0.003
55/45	4.4	3.6	2.6	885	52	364 ± 2	0.859 ± 0.012	0.819 ± 0.002
35/65	3.2	5.9	2.9	643	52	351 ± 9	1.045 ± 0.016	0.767 ± 0.003
19/81	1.9	8.3	3.2	416	54	394 ± 1	1.218 ± 0.010	0.758 ± 0.001

* $R^2 > 0.998$ for all polymer solutions; n is the Power Law exponent

Table S2. Surface zeta potential of membranes.

PAA/PVA	Curing time (min)		
(wt. %)	30	60	120
83/17	-44.5 ± 7.6	-45.6 ± 4.5	-38.1 ± 7.8
55/45	-37.4 ± 2.2	-42.6 ± 4.4	-41.0 ± 5.1
35/65	-35.2 ± 0.2	-40.4 ± 8.2	-40.2 ± 2.3
19/81	-34.5 ± 0.1	-37.9 ± 1.3	n.a

n.a.: not measurable due to fiber characteristics

Table S3a. Toxicity of PAA exposed to *S. aureus* and *E. coli*.

		S. aureus		*E. coli*	
PAA (mg/L)	**pH**	**FDA**	**R_{CFU}**	**FDA**	**R_{CFU}**
0	6.48	100 ± 3	0.00 ± 0.19	100 ± 1	0.00 ± 0.08
0.1	6.48	137 ± 8*	-0.17 ± 0.42	169 ± 16*	0.11 ± 0.06
1	6.48	122 ± 8*	-0.21 ± 0.14*	104 ± 9	0.04 ± 0.07
10	6.42	116 ± 10*	0.06 ± 0.51	99 ± 8	-0.03 ± 0.17
100	6.38	93 ± 13	0.29 ± 0.62	87 ± 11*	0.05 ± 0.07
1000	5.93	61 ± 7*	0.59 ± 0.18*	17 ± 70*	0.20 ± 0.27

FDA bacterial viability: control = 100

$R = \log_{10}(CFU/mL)_{control} - \log_{10}(CFU/mL)_{sample}$

* Statistically significant difference

Table S3b. Toxicity of PVA exposed to *S. aureus* and *E. coli*.

		S. aureus		*E. coli*	
PVA (mg/L)	**pH**	**FDA**	**R_{CFU}**	**FDA**	**R_{CFU}**
0	6.48	100 ± 16	0.00 ± 0.19	100 ± 10	0.00 ± 0.08
0.1	6.47	115 ± 10	-0.07 ± 0.13	111 ± 8	0.06 ± 0.15
1	6.48	103 ± 12	0.05 ± 0.14	100 ± 8	0.04 ± 0.30
10	6.47	114 ± 10	0.05 ± 0.13	100 ± 9	0.11 ± 0.25
100	6.48	92 ± 13	0.08 ± 0.14	96 ± 8	0.12 ± 0.21
1000	6.51	88 ± 14	0.11 ± 0.18	96 ± 9	0.03 ± 0.06

FDA bacterial viability: control = 100

$R = \log_{10}(CFU/mL)_{control} - \log_{10}(CFU/mL)_{sample}$

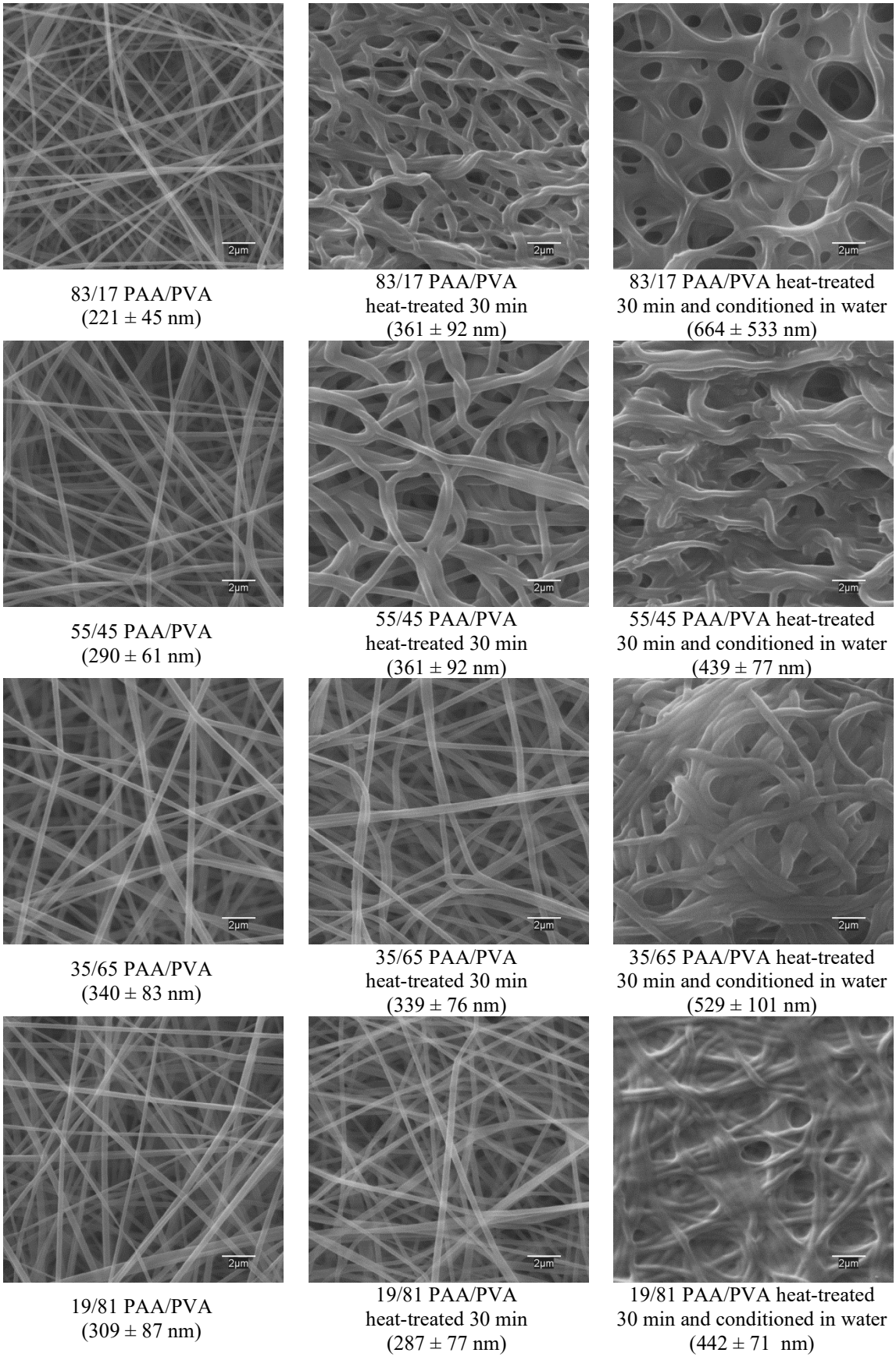

Fig. S1. SEM micrographs and diameters of PAA/PVA fibers freshly electrospun (left), after heat-treating at 140ºC for 30 min (middle), and after water immersion (right)

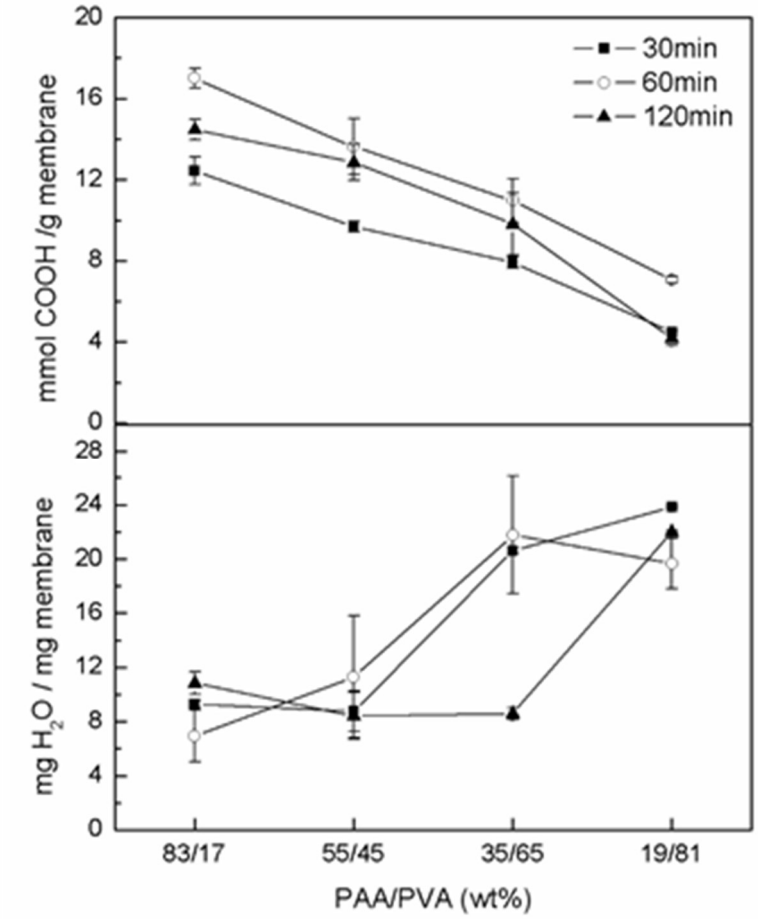

Fig. S2. Carboxylic acid groups on fibers and swelling behavior expressed as water uptake for different PAA/PVA ratio and curing times.

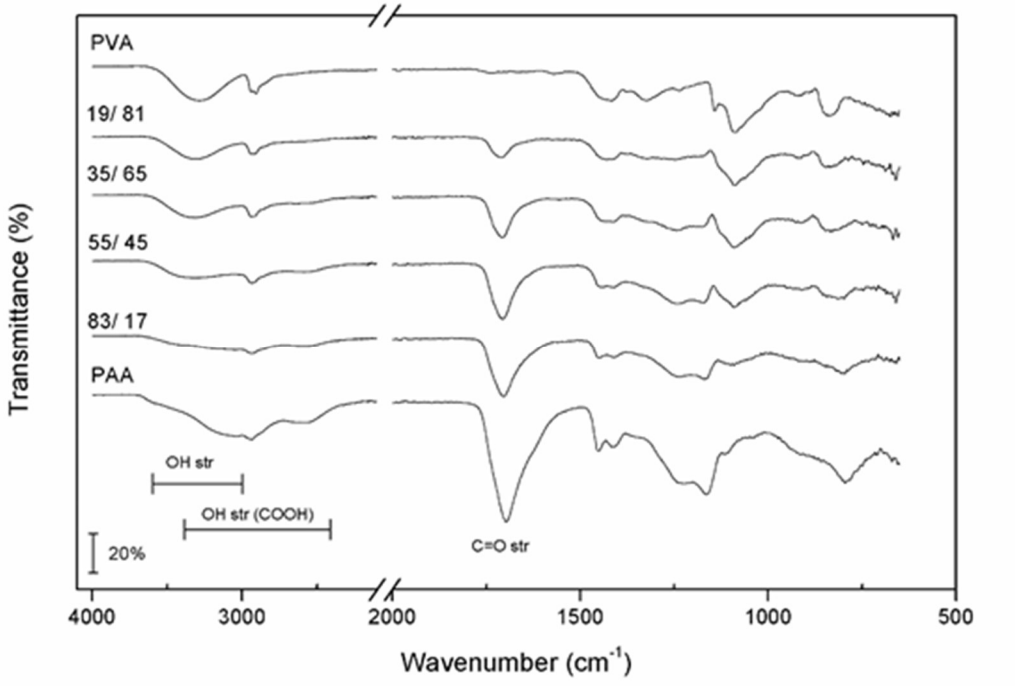

Fig. S3a. ATR- FTIR spectra of freshly electrospun PAA/PVA fibers and pure PAA and PVA.

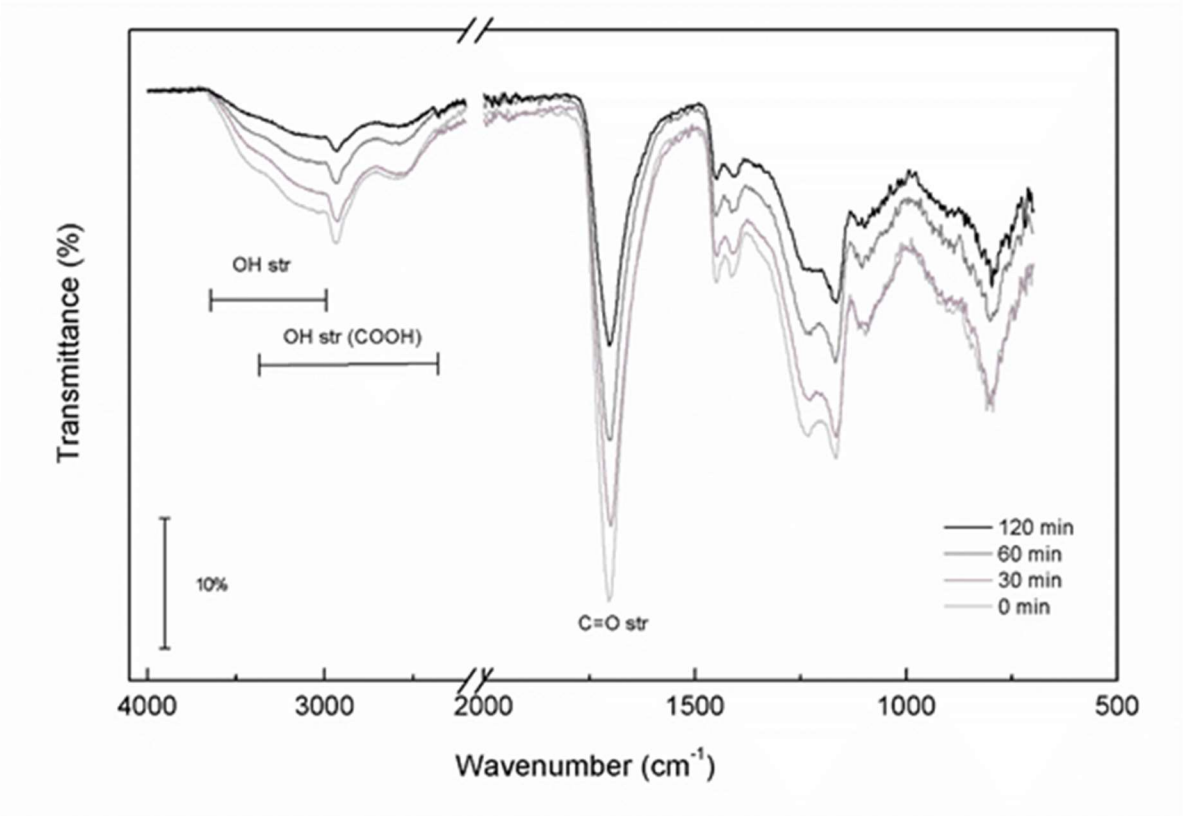

Fig. S3b1. ATR- FTIR spectra of 83/17 PAA/PVA fibers for different curing time.

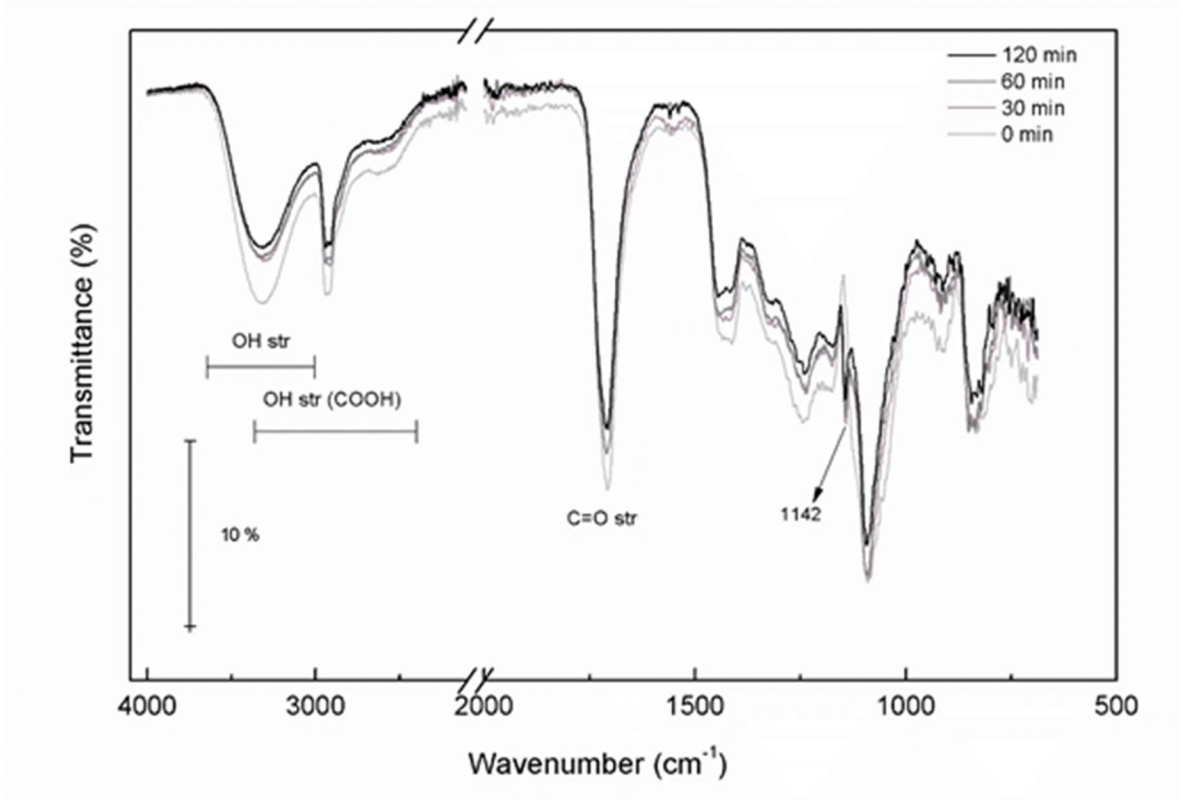

Fig. S3b2. ATR- FTIR spectra of 55/45 PAA/PVA fibers for different curing time.

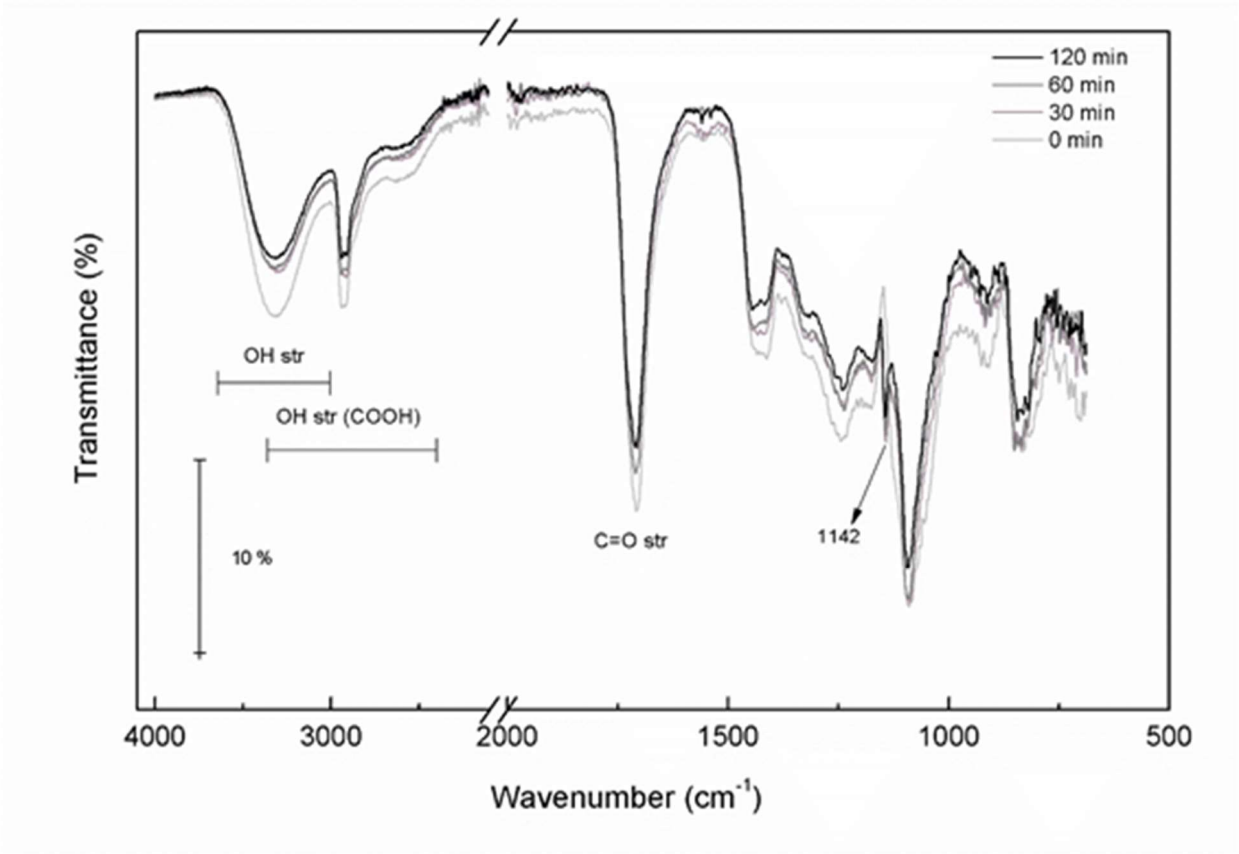

Fig. S3b3. ATR- FTIR spectra of 35/65 PAA/PVA fibers for different curing time.

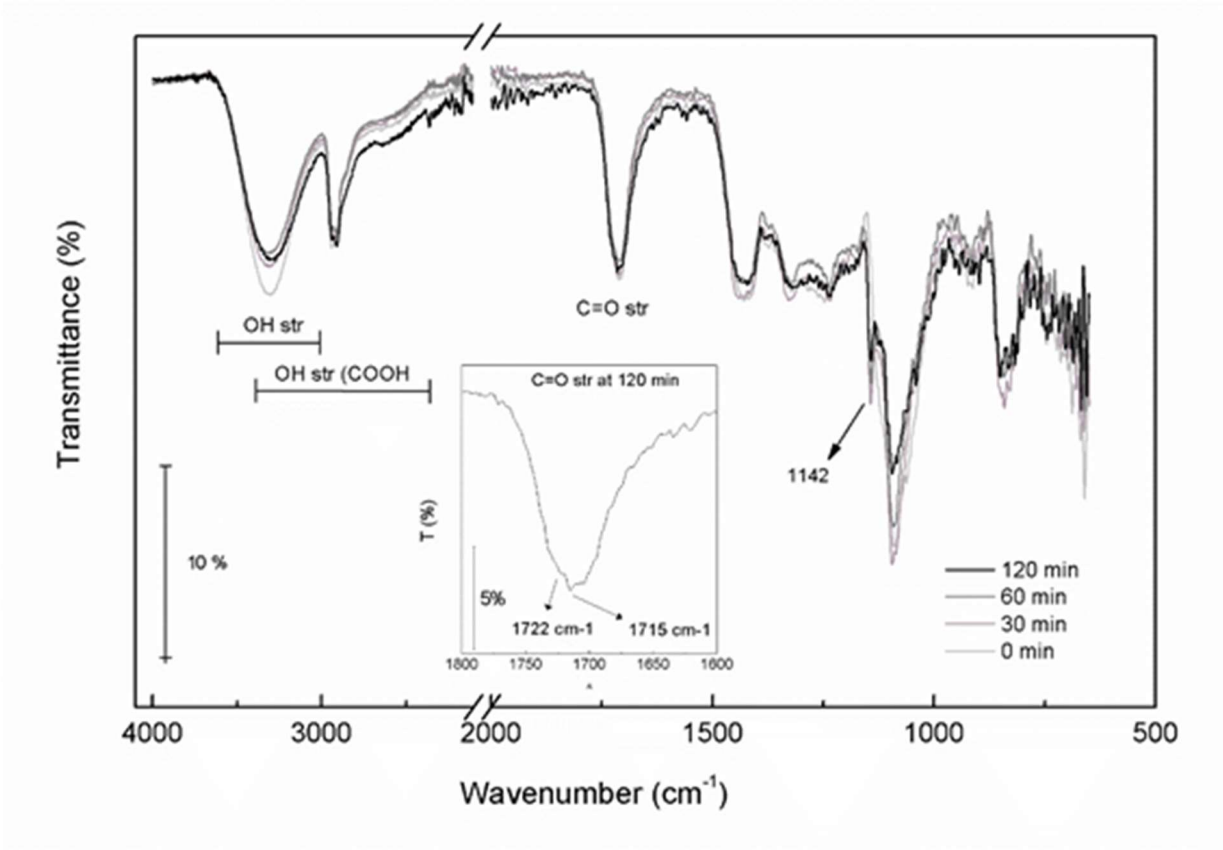

Fig. S3b4. ATR- FTIR spectra of 19/81 PAA/PVA fibers for different curing time.

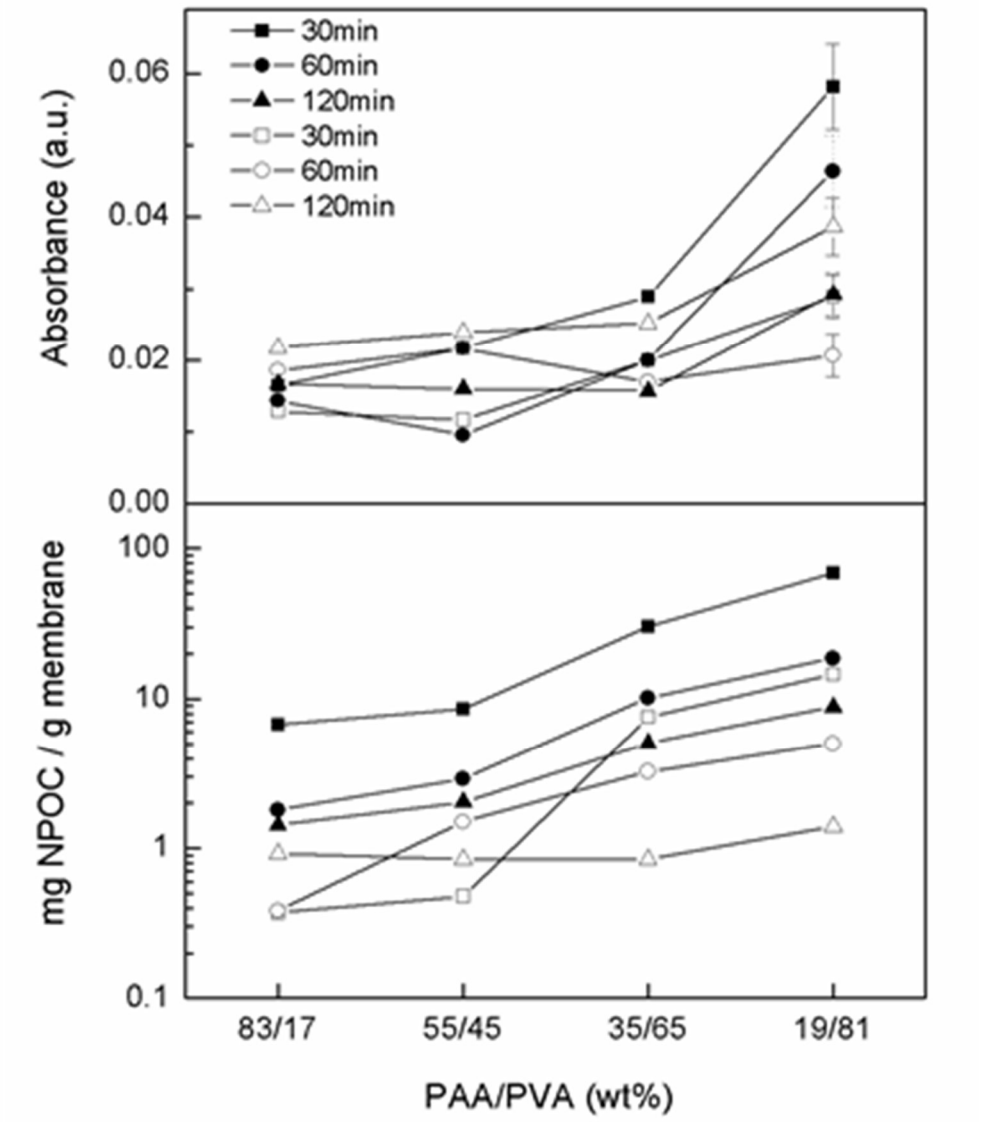

Fig. S4. Polymer release measured as absorbance increase absorbance (a) and NPOC after the first (filled symbols, 24 h) and second water immersion (empty symbols, 24+24 h) for membranes prepared in different conditions.

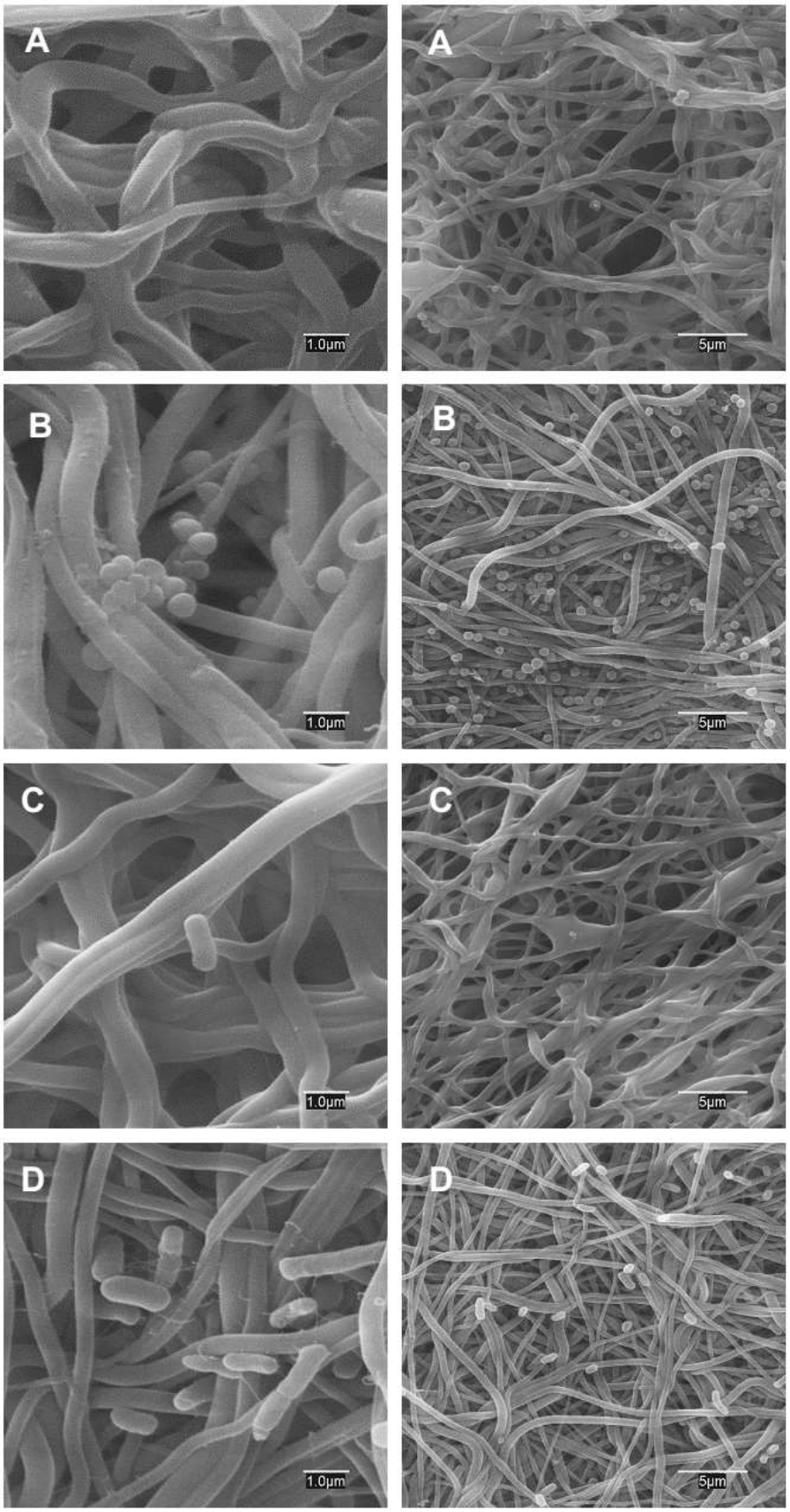

Fig. S5. Fibers of 83/17 (A and C) and 35/65 (B and D) PA/PVA after being 20 h in contact with cultures of *S. aureus* (A and B) and *E. coli* (C and D).

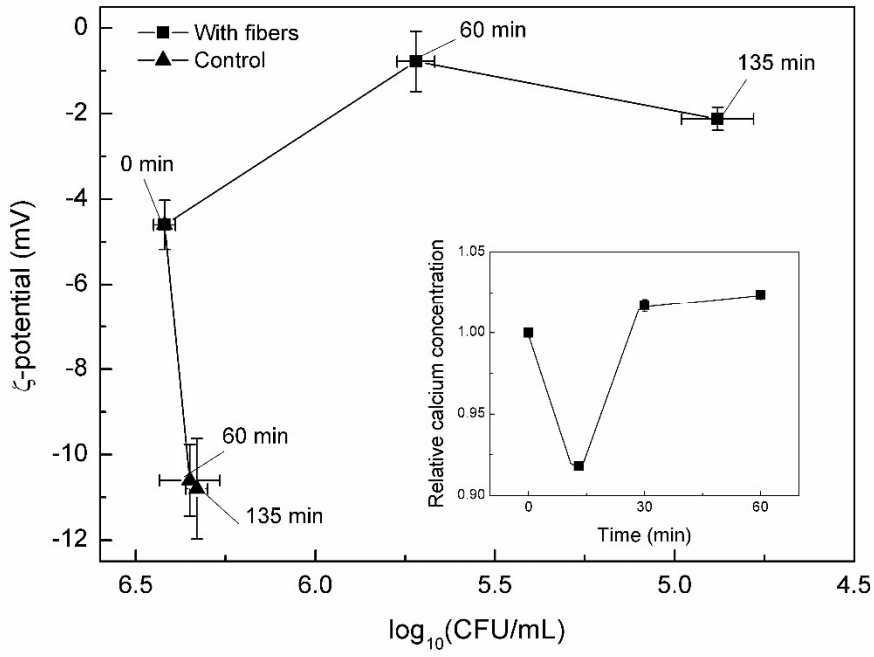

Fig. S6. Changes in ζ-potential of bacteria and colony-forming units (CFU) for *E. coli* exposed to 83/13 PAA/PVA 30 min mat in PBS (■). Control culture in PBS without fibers shown for reference (▲). The inset displays the variation of relative content of intracellular calcium